Sequential assignment and secondary structure determination for the Src homology 2 domain of hematopoietic cellular kinase

Weixing Zhang, Thomas E. Smithgall, William H. Gmeiner*

The Eppley Institute for Research in Cancer and Allied Diseases, The University of Nebraska Medical Center, Omaha, NE 68198-6805, USA

Received 5 December 1996; revised version received 21 February 1997

Abstract The hematopoietic cellular kinase (Hck) is a member of the Src family of non-receptor protein–tyrosine kinases and participates in signal transduction events regulating the growth, differentiation and function of phagocytes. The secondary structure of the SH2 domain for Hck was determined for a $^{13}C/^{15}N$-enriched sample using multi-dimensional NMR spectroscopy. The secondary structure for the domain was determined from chemical shift indices [$^{1}H\alpha$, $^{13}C\alpha$ and $^{13}C'$], sequential NOEs [$d_{\alpha N}(i, i+1)$ and $d_{NN}(i, i+1)$], and $^{3}J_{\alpha N}$ scalar coupling constants. The Hck SH2 domain consists of two α-helices and seven β-strands. Complementary strands of β-sheets were identified from long-range NOEs using a novel 3D, $^{13}C/^{15}N$-edited HMQC-NOESY-(HCACO)NH experiment that correlated $^{1}H\alpha$ resonances between β-strands. The secondary structure for Hck SH2 is similar to that predicted from the sequence alignment of the Src-family protein tyrosine kinases.

Key words: Hck; SH2 domain; Secondary structure; NOESY; Nuclear magnetic resonance

1. Introduction

The hematopoietic cellular kinase (Hck) is a Src-related protein tyrosine kinase that is expressed predominantly in granulocytes, monocytes and macrophages [1–4]. Two isoforms of human Hck (p59 and p61) are produced from a single transcript as a result of alternative sites for translational initiation [5]. Several lines of evidence support specific roles for Hck in functions associated with mature phagocytes. For example, the *hck* gene is strongly activated by agents that induce macrophage differentiation and priming of the respiratory burst [6,7]. Hck has been shown to associate with the Fc receptor and is stimulated in response to receptor activation [8–10]. Thus, Hck may serve as part of a signaling pathway coupling the Fc receptor to the activation of the respiratory burst. Hck has also been implicated in signal transduction by the urokinase plasminogen activator receptor, suggesting that Hck may contribute to neutrophil migration [11]. Finally, the p59 form of Hck localizes predominantly to the secretory granules of human neutrophils, suggesting that it may regulate the degranulation process as well [12].

Further evidence for Hck involvement in neutrophil and macrophage function comes from gene-knockout studies. Hematopoiesis was not detectably impaired in mice with homozygous deletions of Hck, although phagocytosis was affected [13]. Interestingly, the tyrosine kinase activity of Lyn was increased in macrophages from the Hck knock-out animals, suggestive of a possible mechanism to compensate for the loss of Hck. Evidence for functional overlap of Hck with other Src family members comes from analysis of double-mutant animals. For example, mice with homozygous deletions of both Hck and Fgr demonstrated a loss of innate immunity to *Listeria monocytogenes* infection, a pathogen that is normally controlled by macrophages [13]. Similarly, the Hck/Fgr double-knockout animals demonstrated defects in integrin-mediated responses in neutrophils, whereas animals with the individual knockouts showed essentially wild-type responses [14].

Other studies suggest that Hck may contribute to hematopoietic cytokine signal transduction. Hck activation has been reported in response to IL-3, GM-CSF, as well as the gp130-linked cytokine, LIF [15–17]. Overexpression of Hck in IL-3-responsive cells led to a substantial increase in tyrosine phosphorylation following IL-3 treatment [17]. Src was not responsive to IL-3 in similar experiments, indicative of specificity. In the case of LIF, constitutive activation of Hck by gene targeting in embryonic stem cells dramatically reduced the LIF requirement for maintenance of totipotency [16]. Hck was also found to physically associate with gp130, the signal-transducing component of the LIF receptor that is shared with the receptors for IL-6 and other cytokines. These experiments suggest that Hck, together with other members of the Src kinase family, may regulate early embryogenesis.

Hck, and other members of the Src kinase family, share similar structural organization and regulation [18]. The N-terminal region bears sites for lipid attachment, including myristylation and in some cases palmitylation. Both the p59 and p61 forms of Hck are myristylated, whereas only the smaller form is palmitylated. Differential lipid modification may account for the reported differences in subcellular localization of these two isoforms [19]. Adjacent to the N-terminal region are the SH3 and SH2 domains, followed by the kinase domain and negative regulatory tail. The SH2 domain, by virtue of its tyrosine phosphopeptide binding activity, as well as the tail region are essential for negative regulation of tyrosine kinase activity. Tyrosine phosphorylation of a conserved tyrosine residue in this region (Tyr^{527} in Src; Tyr^{501} in Hck) is believed to promote intramolecular interaction of the tail with the SH2 domain, restraining the kinase in an inactive conformation [18]. Dephosphorylation of the tail or displacement of the tail from the SH2 domain as a result of binding to another tyrosine-phosphorylated protein are two possible mechanisms for kinase activation [18]. In this regard, Hck has recently been shown to associate with the p210 form of Bcr/Abl, the oncogenic tyrosine kinase associated with chronic myelogenous leukemia [20]. This association correlated with strong stimulation of Hck tyrosine kinase activity, implicating Hck in Bcr/Abl signal transduction. Activation of Hck may result

*Corresponding author. Fax: (402) 559-4651.
E-mail: bgmeiner@unmc.edu

PII S0014-5793(97)00255-X

from disruption of SH2–tail interaction following binding to tyrosine-autophosphorylated Bcr/Abl. Thus, the SH2 domain of Hck plays a key role in the regulation of tyrosine kinase activity as well as interaction with other proteins. In this report, we provide a complete secondary structural assignment for the Hck SH2 domain, the first structural data to be reported for the Hck protein-tyrosine kinase in solution.

2. Materials and methods

2.1. Sample preparation

The gene segment of *hck* encoding the SH2 domain (residues 119–224) was amplified by PCR from a human *hck* cDNA [1] and inserted into the pET-14b (Novagen) plasmid vector. This vector was used to transform *E. coli* strain BL21(DE3)pLysS. The transformed cells were grown in M9 minimal medium [21] at 37°C. IPTG was added to the growth medium to induce protein expression after the cell density reached ~0.6. Cells were collected by centrifugation 4 h after induction, and lysed by sonication in a buffer containing 50 mM NaCl, 2 mM EDTA, 1% benzamidine, and 20 mM HEPES at pH 7.5. Cell lysates were cleared at 100 000 × *g* and the recombinant SH2 domain (107 residues including the N-terminal methionine from the plasmid vector) in the supernatant was purified using phosphocellulose cation exchange chromatography (P11, Whatman). Further purification was accomplished using gel-filtration chromatography (Sephacryl S-200, Sigma) in 100 mM NaCl, 50 mM sodium phosphate at pH 6.4. Samples of pure protein for NMR spectroscopy were concentrated using Centriprep-3 (Amicon). Isotopically enriched samples were prepared using the same procedure except that $^{15}NH_4Cl$ and [^{13}C]glucose were used as the sole nitrogen and carbon sources, respectively. The molecular weight and amino acid composition of the purified SH2 domain was verified by mass spectrometry and amino acid composition analysis. All samples for NMR analysis were prepared in 90% H_2O/10% D_2O containing 100 mM NaCl, 5 mM DTT-d_{10}, and 50 mM sodium phosphate at pH 6.4 and sealed under argon.

2.2. NMR experiments

All NMR experiments were performed at 28°C using a Varian Unity 500 NMR spectrometer equipped with a triple-resonance pulsed field (z)-gradient probe and amplifier. Sequential assignment of the Hck SH2 domain was accomplished using the CBCA(CO)NH [22] and CBCANH [23] experiments. Ambiguities in resonance assignment due to resonance overlap were resolved using HNCO [24], gd-HCACO [25] and a modified HCA(CO)N [26] experiments. NOEs involving amide protons were assigned using 3D ^{15}N-edited NOESY-HSQC [27], ^{13}C′-edited NOESY-H(N)CO [28], and 4D ^{15}N/^{15}N- and ^{13}C/^{15}N-edited HMQC-NOESY-HSQC [29,30] experiments. NOEs between α-protons were detected using the 3D ^{15}N-edited NOESY-(HCACO)NH experiment [31] and a novel 3D ^{13}C/^{15}N-edited HMQC-NOESY-(HCACO)NH experiment (Fig. 1). Three-bond coupling constants ($^3J_{\alpha N}$) were determined using HNHA [32] and HMQC-*J* [33] experiments. Identification of amide NH in rapid exchange with H_2O was done using the HSQC-exchange experiment [34]. All NMR data were processed with FELIX v2.05 (Hare Research, Inc., Bothel, WA) or NMRPipe [35] using a Sparc-20 workstation.

3. Results and discussion

3.1. Sequential assignments

Sequential resonance assignments were achieved using the 3D CBCA(CO)NH [22] and CBCANH [23] experiments using the procedure described by Grzesiek and Bax [36]. Ambiguities due to overlapped resonances were removed using HNCO [24], gd-HCACO [25] and the HCA(CO)N [26] experiments. The HCA(CO)N pulse sequence was modified to include pulsed field gradient pulses for water suppression. The complete sequential assignment of the amide resonances for the Hck SH2 domain is shown in Fig. 2.

3.2. Identification of secondary structure elements

The secondary structure for the Hck SH2 domain was determined from chemical shift indices [^{1}Hα, ^{13}Cα and ^{13}C′], sequential NOEs [$d_{\alpha N}$(i, i+1) and d_{NN}(i, i+1)], $^3J_{\alpha N}$ scalar coupling constants, and amide proton exchange information (Fig. 3). The chemical shifts for the backbone ^{1}Hα, ^{13}Cα and ^{13}C′ resonances provides information useful for the identification of secondary structural elements of proteins [37]. The ^{13}Cα and ^{13}C′ resonance frequencies are shifted downfield in regions of α-helix compared to random coil values while the ^{1}Hα frequencies are shifted upfield in α-helical regions. The ^{1}Hα, ^{13}Cα and ^{13}C′ backbone resonances also shift in regions of β-sheet relative to random coil values; however, the polarity of the chemical shift changes in this case are opposite to those observed in α-helices.

Sequential NOEs also provides valuable information concerning the secondary structure of proteins [38]. Strong $d_{\alpha N}$(i, i+1) NOEs are observed for regions of β-sheet while these same sequential NOEs are weak in regions of α-helical secondary structure. Conversely, d_{NN}(i, i+1) NOEs are strong in α-helices but weak in regions of β-sheet secondary structure. All possible sequential $d_{\alpha N}$(i, i+1) and d_{NN}(i, i+1) NOEs were observed for the SH2 domain of Hck using a combina-

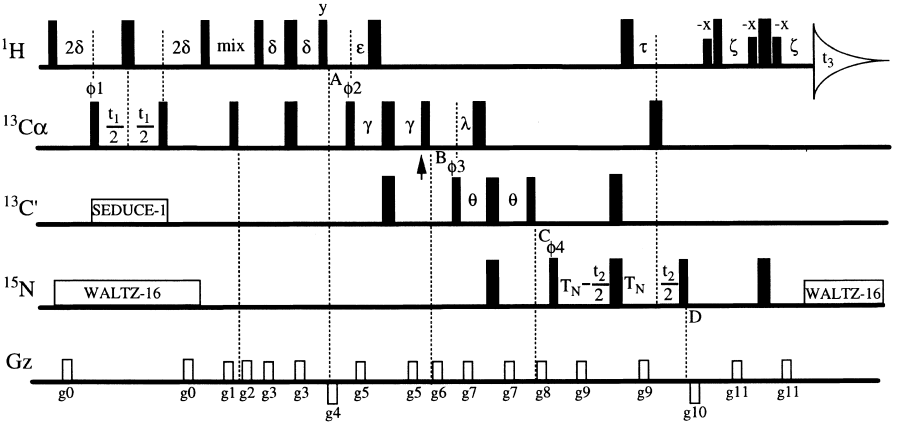

Fig. 1. Pulse sequence of the 3D ^{13}C/^{15}N-edited HMQC-NOESY-(HCACO)NH experiment. Narrow and wide bars represent 90° and 180° pulses, respectively. All pulses are applied along the x-axis unless otherwise indicated. ^{13}C′ decoupling was achieved using the SEDUCE-1 modulation [45] at an RF field strength of 840 Hz. ^{15}N decoupling was accomplished using a WALTZ-16 scheme [46]. The phase cycle is φ1 = x, -x; φ2 = 2x, 2(-x); φ3 = 4x, 4(-x); φ4 = 8x, 8(-x); receiver = x, 2(-x), x, -x, 2x, 2(-x), 2x, -x, x, 2(-x), x. Quadrature detection in t_1 and t_2 is achieved using the States-TPPI method [47] by incrementing the phases of φ1 and φ4, independently. All other parameters are similar to those described for the 3D ^{15}N-edited NOESY-(HCACO)NH experiment [31].

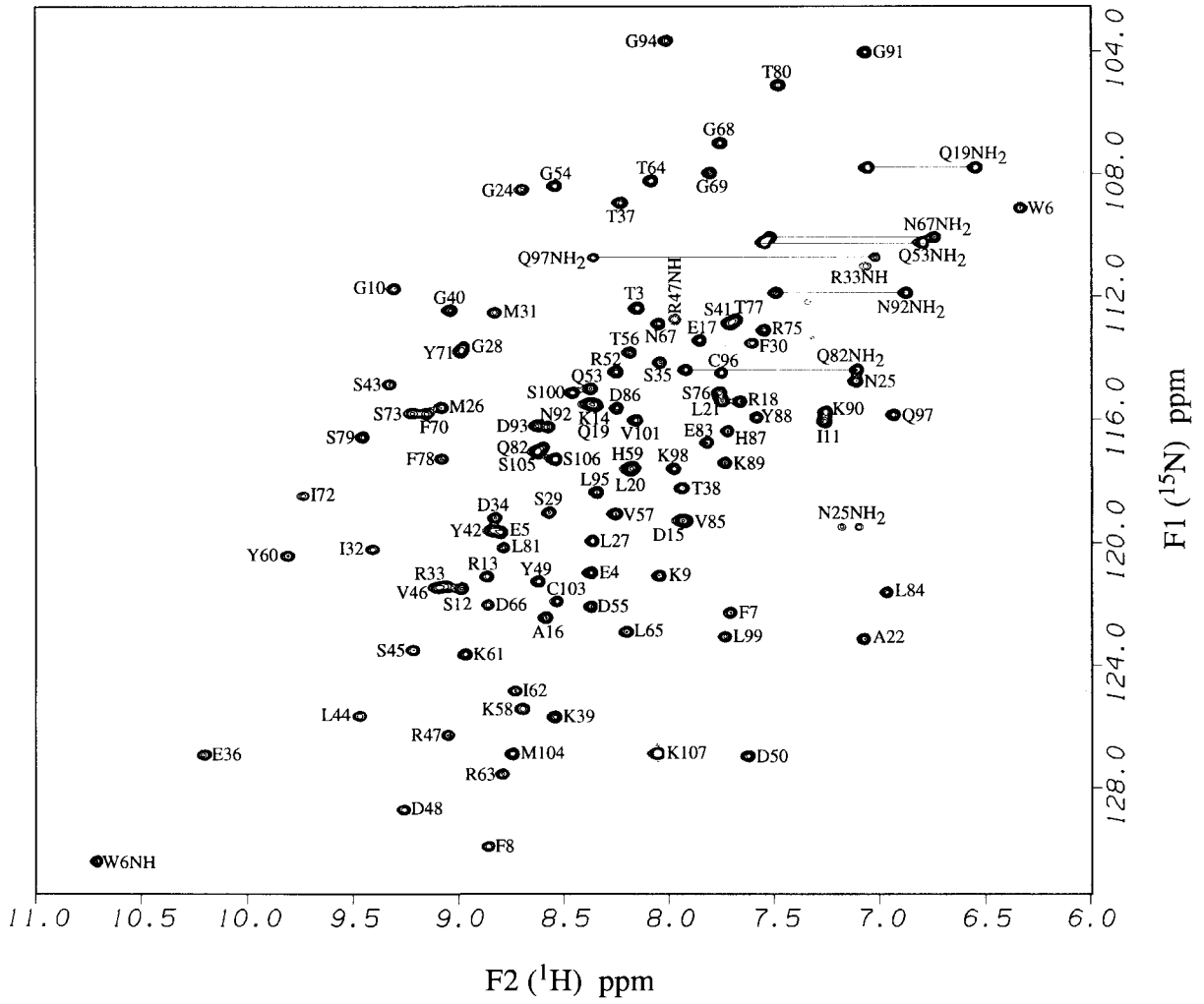

Fig. 2. ^{15}N HSQC spectrum of ^{15}N-labeled Hck SH2, showing assignment of amide resonances. Backbone resonances are labeled with the residue name followed by residue number in the sequence. Side chain NH of Trp and Arg are indicated with NH while side chain NH_2 of Asn and Gln are indicated by NH_2.

tion of 3D ^{15}N-edited NOESY-HSQC [27], ^{13}C′-edited NOESY-H(N)CO [28], and 4D ^{15}N/^{15}N- and ^{13}C/^{15}N-edited HMQC-NOESY-HSQC [29,30] experiments. The results are presented in Fig. 3.

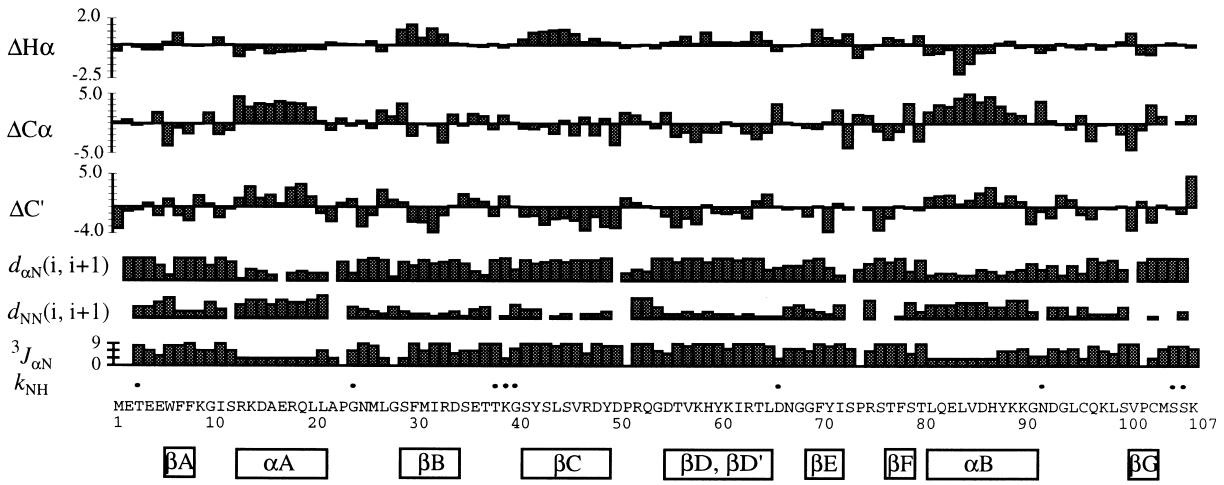

Fig. 3. Summary of sequentially dependent data of Hck SH2. ΔHα, ΔCα, and ΔC′ are the deviations of chemical shifts from random coil values for ^{1}Hα, ^{13}Cα, and ^{13}C′, respectively. $d_{\alpha N}$(i, i+1) and d_{NN}(i, i+1) are sequential NOEs between residues i and i+1. $^{3}J_{\alpha N}$ is the scalar coupling constant between ^{1}Hα and backbone $^{1}H_N$. k_{NH} indicates amide protons which are in fast exchange with water in the HSQC-exchange experiment [34].

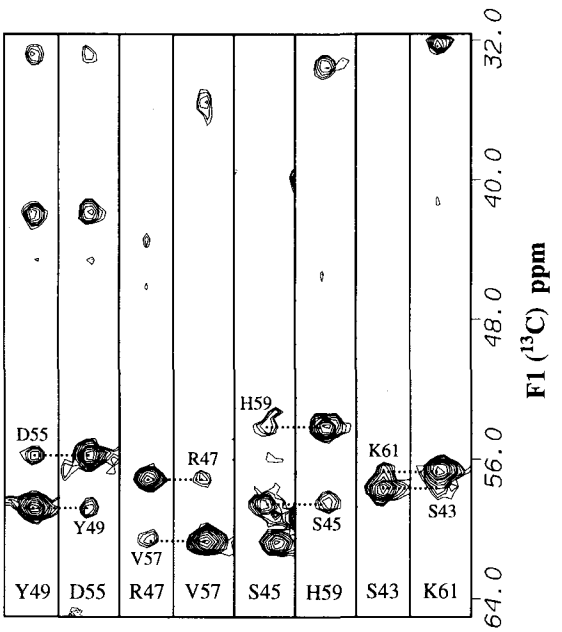

^{1}Hα	4.74	4.87	4.57	4.75	5.60	5.53	5.47	4.56	ppm
F2 (^{15}N)	126.9	113.4	128.7	125.4	121.6	120.4	125.6	124.8	ppm
F3 (^{1}H)	7.62	8.18	9.25	8.69	9.10	9.80	9.46	8.72	ppm

Fig. 4. F1 strips from the 3D ^{13}C/^{15}N-edited HMQC-NOESY-(HCACO)NH spectrum of Hck SH2, showing four pairs of $d_{\alpha\alpha}$(i, j) NOEs in antiparallel β-sheet region. The data were obtained from a 48(t_1)×32(t_2)×512(t_3) complex matrix with a spectrum width of 6283, 1500, and 6000 Hz, respectively. A 16-step phase cycle and a relaxation delay of 0.8 s were used. The mixing period was 100 ms.

The $^3J_{\alpha N}$ scalar coupling constant is a function of the backbone dihedral angle (φ) and is therefore dependent on protein secondary structure [38]. Residues involved in α-helical regions are characterized by small values of $^3J_{\alpha N}$ (< 6 Hz) while those embedded in β-sheet have characteristically large values of $^3J_{\alpha N}$ (> 8 Hz). The $^3J_{\alpha N}$ scalar coupling constants for the Hck SH2 domain were evaluated using HNHA [32] and HMQC-*J* [33] experiments. The results are presented in Fig. 3. Excellent correlation is observed between residues with small values of $^3J_{\alpha N}$ and those with sequential NOEs and chemical shift indices characteristic of α-helical secondary structure. Analogous results were also obtained for regions of β-strand secondary structure. Amide proton exchange rates [34] also give information useful for the identification of secondary structural elements. In particular, residues having fast exchange rates for backbone ^1H_N are normally located outside regions of well-defined α-helical or β-strand secondary structure. A depiction of those backbone ^1H_N that are in rapid exchange with solvent is also included in Fig. 3.

The location and nature of secondary structure elements for the Hck SH2 domain were identified by combining information from chemical shift indices [^{1}Hα, ^{13}Cα and ^{13}C′], sequential NOEs [$d_{\alpha N}$(i, i+1) and d_{NN}(i, i+1)], $^3J_{\alpha N}$ scalar coupling constants, and amide proton exchange rates (Fig. 3). The Hck SH2 domain consists of two α-helices (residues 13–21 and 81–91) and seven β-strands (residues 6–8, 29–34, 41–49, 55–65, 69–72, 77–79, 81–91, and 101–103). The number and spacing of these secondary structural elements is similar to those reported for other SH2 domains.

Identification of partner β-strands comprising a β-sheet requires assignment of long-range NOEs [$d_{\alpha\alpha}$(i, j), $d_{\alpha N}$(i, j) and d_{NN}(i, j)]. Determination of NOEs between ^{1}Hα unambiguously in water is a challenging task since some ^{1}Hα may resonate exactly at the ^1H_2O frequency. In order to overcome this difficulty, a novel 3D ^{13}C/^{15}N-edited HMQC-NOESY-(HCACO)NH experiment was developed. The pulse sequence for this experiment is shown in Fig. 1. In this experiment, the ^{1}Hα from which the NOE originates is edited by the ^{13}Cα chemical shift while the dipolar coupled ^{1}Hα partner that is the destination of the NOE is correlated to the ^{15}N chemical shift in the succeeding residue. Fig. 4 shows some of the F1

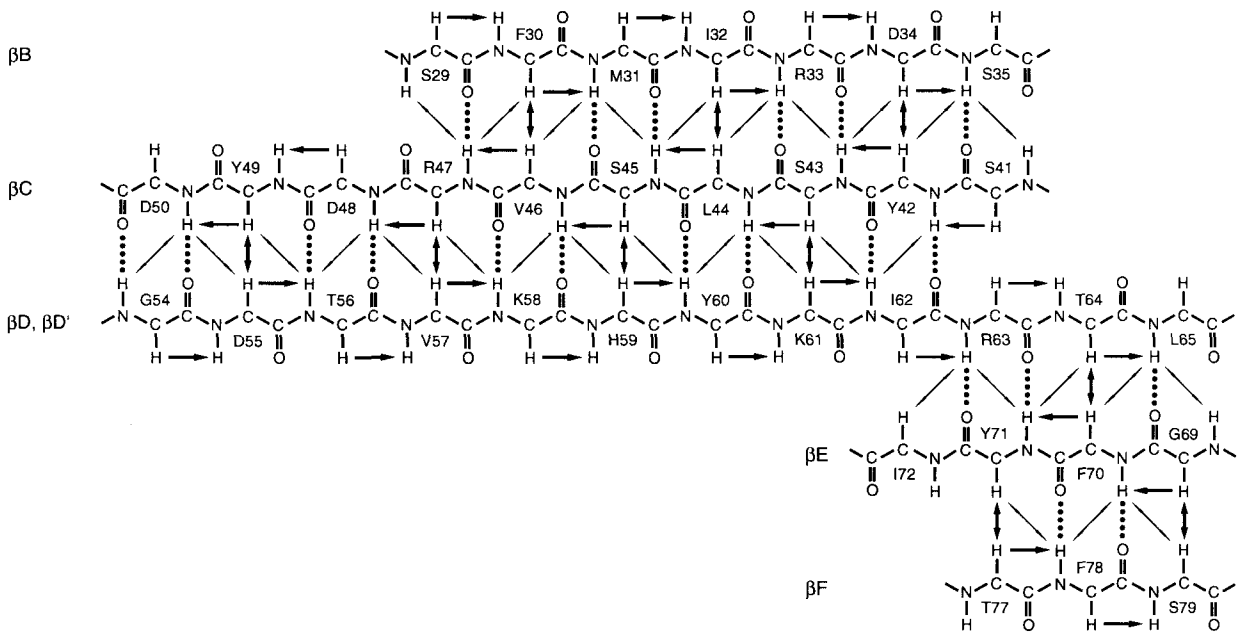

Fig. 5. Schematic diagram of the antiparallel β-sheet region of the Hck SH2 domain. Solid arrows indicate observed long-range NOEs. Arrow width indicates relative NOE intensity. Dashed lines represent possible hydrogen bonds which are consistent with observation of slowly exchanging amide protons.

strips of the 3D $^{13}C/^{15}N$-edited HMQC-NOESY-(HCACO)NH spectrum for the Hck SH2 domain. Combined use of this new experiment with the 3D ^{15}N-edited NOESY-(HCACO)NH experiment [31], allowed unequivocal assignment for all $d_{\alpha\alpha}(i, j)$ NOEs in the anti-parallel β-sheets. A summary of the experimentally observed long-range NOEs in the anti-parallel β-sheet segments is presented in Fig. 5. Strong NOEs are indicated by thick arrows while medium NOEs are shown with thin arrows.

Structures derived from heteronuclear multidimensional NMR data have been reported for the SH2 domains of c-Abl [39], the C-terminal SH2 domain of PLC-γl [40], Crk [41], the N-terminal SH2 domain of PI 3′ kinase [42], c-Src [43] and Blk [44]. In this report, we present the resonance assignments and secondary structure determination for the SH2 domain of the Src-family protein tyrosine kinase, Hck. Structural information concerning the Hck SH2 domain is essential both to enrich our understanding of the structural basis for SH2-ligand interactions, and also to understand the structural basis for signal transduction mediated by Hck, a protein that plays unique roles in the regulation of the growth, differentiation, and function of phagocytes (see Section 1).

4. Conclusions

The sequential resonances for the Hck SH2 domain have been assigned and the secondary structure elements for this domain have been identified. The overall topology of the Hck SH2 domain is similar to that reported previously for the SH2 domain of c-Src and consists of two α-helices and seven β-strands. The development of a novel 3D, $^{13}C/^{15}N$-edited HMQC-NOESY-HCACO(NH) experiment permitted the unambiguous assignments for all the strong $d_{\alpha\alpha}(i, j)$ NOEs in the antiparallel β-sheets. The secondary structure information, along with a high resolution 3D structure, will be helpful in understanding the function of this domain critical for negative regulation and substrate recognition of Hck. Refinement of the 3D structure of Hck SH2 domain is in progress in our laboratory.

Acknowledgements: This research was supported in part by grants from the National Institute of Health (NIH-NCI CA-36727, NIH-NCI CA58667 [T.E.S.]), the American Cancer Society (IRG-165G [W.H.G.]) and the Nebraska Department of Health [W.H.G.]. We thank Dr. R. Andrew Byrd at the ABL Macromolecular Structure Laboratory in Frederick, MD, for his help with some of the NMR experiments, Dr. Fulvio Perini for amino acid analysis, David Babcook for NMR instrumental assistance, and Scott D. Briggs for assistance with molecular cloning.

References

[1] S.F. Ziegler, J.D. Marth, D.B. Lewis, R.M. Perlmutter, Mol Cell Biol 7 (1987) 2276–2285.
[2] N. Quintrell, R. Lebo, H. Varmus, J.M. Bishop, M.J. Pettenati, M.M. Le Beau, M.O. Diaz, Mol Cell Biol 7 (1987) 2267–2275.
[3] D.A. Holtzman, W.D. Cook, A.R. Dunn, Proc Natl Acad Sci USA 84 (1987) 8325–8329.
[4] M.J. Klemsz, S.R. McKercher, R.A. Maki, Nuc Acids Res 15 (1987) 9600–9602.
[5] P. Lock, S. Ralph, E. Stanley, I. Boulet, R. Ramsay, A.R. Dunn, Mol Cell Biol 11 (1991) 4363–4370.
[6] I. Boulet, S. Ralph, E. Stanley, P. Lock, A.R. Dunn, S.P. Green, W.A. Phillips, Oncogene 7 (1992) 703–710.
[7] U. Lichtenberg, N. Quintrell, J.M. Bishop, Oncogene 7 (1992) 849–858.
[8] S. Ghazizadeh, J.B. Bolen, H.B. Fleit, J Biol Chem 269 (1994) 8878–8884.
[9] A.V. Wang, P.R. Scholl, R.S. Geha, J Exp Med 180 (1994) 1165–1170.
[10] D.L. Durden, H.M. Kim, B. Calore, Y. Liu, J Immunol 154 (1995) 4039–4047.
[11] J. Bohuslav, V. Horejsi, C. Hansmann, J. Stockl, U.H. Weidle, O. Majdic, I. Bartke, W. Knapp, H. Stockinger, J Exp Med 181 (1995) 1381–1390.
[12] H. Möhn, V. Le Cabec, S. Fischer, I. Maridonneau-Parini, Biochem J 309 (1995) 657–665.
[13] C.A. Lowell, P. Soriano, H.E. Varmus, Genes Dev 8 (1994) 387–398.
[14] C.A. Lowell, L. Fumagalli, G. Berton, J Cell Biol 133 (1996) 895–910.
[15] D. Linnekin, O.M.Z. Howard, L. Park, W. Farrar, D. Ferris, D.L. Longo, Blood 84 (1994) 94–103.
[16] M. Ernst, D.P. Gearing, A.R. Dunn, EMBO J 13 (1994) 1574–1584.
[17] S.M. Anderson, B. Jorgensen, J Immunol 155 (1995) 1660–1670.
[18] M.T. Brown, J.A. Cooper, Biochim Biophys Acta 1287 (1996) 121–149.
[19] S.M. Robbins, N.A. Quintrell, J.M. Bishop, Mol Cell Biol 15 (1995) 3507–3515.
[20] S. Danhauser-Riedl, M. Warmuth, B.J. Druker, B. Emmerich, M. Hallek, Cancer Res 56 (1996) 3589–3596.
[21] Sambrook, J., Fritsch, E.F. and Maniatis, T. (1989) Molecular Cloning: a Laboratory Manual, 2nd edn., Cold Spring Harbor Laboratory Press, New York.
[22] S. Grzesiek, A. Bax, J Am Chem Soc 114 (1992) 6291–6293.
[23] S. Grzesiek, A. Bax, J Magn Reson 99 (1992) 201–207.
[24] D.R. Muhandiram, L.E. Kay, J Magn Reson Ser B 103 (1994) 203–216.
[25] W. Zhang, W.H. Gmeiner, J Biomol NMR 7 (1996) 247–250.
[26] R. Powers, A.M. Gronenborn, G.M. Clore, A. Bax, J Magn Reson 94 (1991) 209–213.
[27] O. Zhang, L.E. Kay, J.P. Olivier, J.D. Forman-Kay, J Biomol NMR 4 (1994) 845–858.
[28] W. Zhang, T.E. Smithgall, W.H. Gmeiner, J Magn Reson Ser B 111 (1996) 305–309.
[29] M. Ikura, A. Bax, G.M. Clore, A.M. Gronenborn, J Am Chem Soc 112 (1990) 9020–9022.
[30] D.R. Muhandiram, G.Y. Xu, L.E. Kay, J Biomol NMR 3 (1993) 463–470.
[31] W. Zhang, W.H. Gmeiner, J. Biomol. NMR 8 (1996) 357–359.
[32] G.W. Vuister, A. Bax, J Am Chem Soc 115 (1993) 7772–7777.
[33] L.E. Kay, A. Bax, J Magn Reson 86 (1990) 110–126.
[34] S. Grzesiak, A. Bax, J Biomol NMR 3 (1993) 627–638.
[35] F. Delaglio, S. Grzesiek, G.W. Vuister, G. Zhu, J. Pfeifer, A. Bax, J Biomol NMR 6 (1995) 277–293.
[36] S. Grzesiek, A. Bax, J Biomol NMR 3 (1993) 185–204.
[37] D.S. Wishart, B.D. Sykes, Methods Enzymol 239 (1994) 363–392.
[38] Wüthrich, K. (1986) NMR of Proteins and Nucleic Acids, John Wiley, New York.
[39] M. Overduin, C.B. Rios, B.J. Mayer, D. Baltimore, D. Cowburn, Cell 70 (1992) 697–704.
[40] S.M. Pascal, A.U. Singer, G. Gisg, T. Yamazaki, S.E. Shoelson, T. Pawson, L.E. Kay, J.D. Forman-Kay, Cell 77 (1994) 461–472.
[41] M.K. Rosen, T. Yamazaki, G.D. Gish, C.M. Kay, T. Pawson, L.E. Kay, Nature 374 (1995) 477–479.
[42] M. Hensmann, G.W. Booker, G. Panayotou, J. Boyd, J. Linacre, M. Watefield, I.D. Campbell, Prot Sci 3 (1994) 1020–1030.
[43] R.J. Boerner, T.G. Consler, R.T. Gampe Jr., D. Weigl, D.H. Willard, D.G. Davis, A.M. Edison, F. Loganzo Jr., D.B. Kassel, R.X. Xu, I.R. Patel, J.S. Robbins, T. Lansing, T.M. Gilmer, M.A. Luther, W.B. Knight, Biochemistry 34 (1995) 15351–15358.
[44] W.J. Metzler, B. Leiting, K. Pryor, L. Mueller, B.T. Farmer II, Biochemistry 35 (1996) 6201–6211.
[45] M.A. Mccoy, L. Mueller, J Am Chem Soc 114 (1992) 2108–2112.
[46] A.J. Shaka, J. Keeler, T. Frenkiel, R. Freeman, J Magn Reson 52 (1983) 335–338.
[47] D. Marion, M. Ikura, R. Tschudin, A. Bax, J Magn Reson 85 (1989) 393–399.